Taylor & Francis
Taylor & Francis Group

Inhalation Toxicology

International Forum for Respiratory Research

ISSN: 0895-8378 (Print) 1091-7691 (Online) Journal homepage: http://www.tandfonline.com/loi/iiht20

Modelling of individual subject ozone exposure response kinetics

Edward S. Schelegle, William C. Adams, William F. Walby & M. Susan Marion

To cite this article: Edward S. Schelegle, William C. Adams, William F. Walby & M. Susan Marion (2012) Modelling of individual subject ozone exposure response kinetics, Inhalation Toxicology, 24:7, 401-415

To link to this article: http://dx.doi.org/10.3109/08958378.2012.683891

Inhalation Toxicology, 2012; 24(7): 401–415
© 2012 Informa Healthcare USA, Inc.
ISSN 0895-8378 print/ISSN 1091-7691 online
DOI: 10.3109/08958378.2012.683891

informa
healthcare

MODELING/SYMMETRY

Modelling of individual subject ozone exposure response kinetics

Edward S. Schelegle[1], William C. Adams[2], William F. Walby[1], and M. Susan Marion[3]

[1]*Department of Anatomy, Physiology and Cell Biology, University of California, School of Veterinary Medicine, Davis, CA, USA,* [2]*Department of Exercise Biology, University of California, Davis, CA, USA, and* [3]*California National Primate Research Center, University of California, Davis, CA, USA*

Abstract

Context: A better understanding of individual subject ozone (O_3) exposure response kinetics will provide insight into how to improve models used in the risk assessment of ambient ozone exposure.

Objective: To develop a simple two compartment exposure–response model that describes individual subject decrements in forced expiratory volume in one second (FEV_1) induced by the acute inhalation of O_3 lasting up to 8 h.

Methods: FEV_1 measurements of 220 subjects who participated in 14 previously completed studies were fit to the model using both particle swarm and nonlinear least squares optimization techniques to identify three subject-specific coefficients producing minimum "global" and local errors, respectively. Observed and predicted decrements in FEV_1 of the 220 subjects were used for validation of the model. Further validation was provided by comparing the observed O_3-induced FEV_1 decrements in an additional eight studies with predicted values obtained using model coefficients estimated from the 220 subjects used in cross validation.

Results: Overall the individual subject measured and modeled FEV_1 decrements were highly correlated (mean R^2 of 0.69 ± 0.24). In addition, it was shown that a matrix of individual subject model coefficients can be used to predict the mean and variance of group decrements in FEV_1.

Conclusion: This modeling approach provides insight into individual subject O_3 exposure response kinetics and provides a potential starting point for improving the risk assessment of environmental O_3 exposure.

Keywords: Ozone, exposure–response model, human

Introduction

Ozone is the primary oxidant found in photochemical air pollution and is one of the six criteria for air pollutants identified in the 1971 United States Clean Air Act. The O_3 exposure–response relationship has been examined in controlled clinical studies in which individuals are exposed to multiple O_3 concentrations while varying duration of exposure, and minute ventilation (V_E). Several investigators (Adams et al., 1981, Hazucha, 1987, McDonnell et al., 1983, McDonnell et al., 1997, McDonnell et al., 2007) have used measurements of forced expiratory volume in one second (FEV_1) as well as other markers of response to derive empirical exposure-response models with the goal of estimating population responses to ambient exposures. An observation from the earlier 2.5 hour clinical studies was that increasing the total inhaled dose or "effective dose" expressed as the product of O_3 concentration, time, and minute ventilation would increase pulmonary function decrements, rapid shallow breathing rates, and subjective symptoms (Silverman et al., 1976, Folinsbee et al., 1978, McDonnell et al., 1983, Adams et al., 1981). In addition, based on the observations of Hazucha el al. (1973) of a nonlinear relationship between ozone concentration and pulmonary function decrements, mean exposure–response data was fit to

Address for Correspondence: Edward S. Schelegle, Department of Anatomy, Physiology and Cell Biology, University of California, 1 Shields Avenue, Davis, CA 95616, USA. Tel.: +530 752-1177. Fax: +530 752–7690. E-mail: esschelegle@ucdavis.edu

(Received 22 September 2011; revised 29 March 2012; accepted 05 April 2012)

polynomial and multiple regression models (Silverman et al., 1976, Folinsbee et al., 1978, McDonnell et al., 1983, Adams et al., 1981). Though useful in predicting mean O_3-induced FEV_1 decrements in exposures of short duration, effective dose has several limitations in simulating mean responses to longer duration exposures and those with more realistic variable O_3 concentration and minute ventilation profiles typical of actual human exposures.

Subsequently, McDonnell et al. (1997, 1999, 2007, and 2010) began an effort to develop a predictive model of mean O_3-induced FEV_1 response that uses a sigmoid function, compartmentalization and allows changes in O_3 concentration and V_E during exposure of varying duration. McDonnell et al's model is consistent with the group mean responses previously observed during 2.5 and 6.6 h protocols using O_3 concentrations ranging from 80 to 400 ppb (McDonnell et al., 1983). The model consists of two compartments (McDonnell et al., 1999). In the first compartment the concentration of a substance, *X*, that activates airway afferent nerves increases at the rate ozone is inhaled ($[O_3] \times V_E$) and decreases at the rate that *X* is cleared or metabolized. In the second compartment the decrement in FEV_1 increases as a sigmoid-shaped function of [*X*] with age (McDonnell et al., 1997, 1999, 2007) and body mass index (McDonnell et al., 2010). This modifies the relationship between [*X*] and the change in FEV_1, approaching a fixed asymptote.

All of the modelling approaches to date predict a progressive decrement in FEV_1 starting at the beginning of O_3 exposure. However, the prediction of the onset of response at the beginning of exposure is contrary to the anecdotal reports of participants in O_3 inhalation studies that describe a period of exposure that precedes the onset of symptoms suggesting a delay in onset of O_3-induced response. Further support for the existence of a delay in onset of O_3-induced responses is provided in the exposure–response study of Adams et al. (1981). Plots of percent change in respiratory rate, mid-maximal flow rate, forced vital capacity and FEV_1 against effective dose all show that the onset of response does not occur until the effective dose exceeds 400 ppm × L or 780 μg of O_3 (Adams et al., 1981). Schelegle et al. (1989) report that O_3 sensitive subjects who inhaled 200 ppb O_3 in two consecutive 40 min intervals with V_E set at 50 L/min did not have significant alterations in pulmonary function and symptoms after the first 40 min period (effective dose 400 ppm × L or 780 μg of O_3) but did have significant decrements in function and symptoms after the second exposure interval. We systematically addressed this question using a retrospective analysis of individual subject breathing pattern data that was recorded during continuous exercise exposure protocols (Schelegle et al., 2007). This analysis resulted in three important observations. First, the onset of O_3-induced rapid shallow breathing demonstrates a clear dose of onset of response (Dos) for each subject that was not influenced by changes in ozone concentration. Second, the magnitude of the O_3-induced tachypnea, that developed after Dos was reached, was not correlated with the value of Dos. Third, while the magnitude of the O_3-induced tachypnea was variable between subjects, it was proportional to the inhaled dose rate (μg O_3/min) within a subject. Subsequently, we demonstrate Dos for FEV_1 in a group of subjects, who completed a series of prolonged 6.6 h O_3 exposures (Schelegle et al., 2009). In the current analysis, we continued this effort and extended our investigation to how combined individual kinetics and responsiveness interact to produce the mean FEV_1 response and the associated skewed distribution of FEV_1 response seen in human exposure response studies (McDonnell et al., 1983, Kulle et al., 1985). Our goal is to identify coefficients that better characterize individual O_3 response kinetics and responsiveness that can be used in future genomic and metabolomic analysis, as well as, identify how current predictive models might be modified to better reflect individual subject kinetics.

Our approach has been to consider a single breath as the minimum unit of exposure, with tidal volume and ozone concentration determining the dose of ozone inhaled in that breath. An exposure protocol consists of a series of successive breaths, with an individual's kinetics of response being represented by the dose of onset and the kinetics of the response once this onset is reached. Since responses to ozone have been shown to be reproducible within a subject, multiple exposures can be used to better define the kinetics of response in a single subject. The response of a group of subjects to a given exposure regimen is the result of the combined responses of the individuals in the group, each with their own kinetics of response. The variance of response of a group to a given exposure regimen is the result of each individuals kinetics of response (i.e. what phase of response is the subject at the time of measurement) and the factors that determine the responsiveness of each individual. Responsiveness is defined as the maximum response that can be generated by a subject at a fixed dose rate of exposure. Group effects arise as a consequence of the interaction between kinetic and responsiveness factors. Such a group effect is the sigmoid function incorporated into the model of McDonnell et al. (1997).

In order to fit individual subject FEV_1 data, we use the simplest model possible that contains two compartments and three coefficients and is consistent with our previous analysis of the onset and magnitude of O_3-induced tachypnea (Schelegle et al., 2007). The first compartment represents the dose of onset or Dos and is modelled essentially as a square wave. The second compartment is identical to the first compartment of McDonnell et al's model (McDonnell et al., 1997), and models a single compartment of fixed volume with a constant rate of elimination of a bioactive substance that activates the deep lung neural receptors that induce ozone-induced rapid shallow breathing and reductions in inspiratory capacity (i.e. decreased FEV_1). The output of these two compartments is then multiplied by a proportionality or responsiveness coefficient A.

Methods

Source data

FEV_1 measurements from 704 healthy, non-smoking subjects (628 males and 76 females), 18–35 years of age were obtained from 91 different protocols (29 filtered air and 62 O_3 exposure protocols) from 21 different studies (18 published; Table 1). These studies were conducted at the EPA exposure chambers on the University of North Carolina Chapel Hill campus between 1980 and 1993 (Folinsbee et al., 1988, Horstman et al., 1990, 1995, Kehrl et al., 1987, Koren et al., 1989, McDonnell, 1983, 1987, 1989, 1991, Seal et al., 1993) and the exposure facilities in the Human Performance Laboratory on the University of California Davis campus between 1996 and 2008 (Adams, 2000a, 2000b, 2002, 2003a, 2003b, 2006a, 2006b, Adams & Ollison, 1997, Schelegle et al., 2009). In addition, data from three unpublished studies (two resting protocols and one heavy intermittent exercise protocol) were contained in the EPA exposure dataset. In one of the resting studies, 70 subjects were exposed for 2.5 h to 0 ($n = 5$), 120 ($n = 1$), 180 ($n = 13$), 240 ($n = 17$), 300 ($n = 12$) or 400 ($n = 22$) ppb O_3, while in the other resting study 16 subjects were exposed to 0, 120, 180, and 240 ppb O_3. In the unpublished heavy

Table 1. List of published studies from which data was obtained.

	Volunteers			Exposure characteristics				
Study	*n*	Age (years)	BSA (m^2)	Type	Pattern	Duration (h)	Mean C (ppb)	Target EVR
Adams (2006a, 2006b)*	15 M	23.5	1.98	CH	SW	8.0	FA, 120	20
	15 F	22.8	1.65	CH	RAMP	8.0	120	20
	15 M	23.5	1.98	CH	SW	6.6	FA, 60, 80	20
	15 F	22.8	1.65	CH	STEP	w	40, 60, 80	20
Adams (2002)*	15 M	22.2	1.93	CH	SW	6.6	FA, 120	20
	15 F	22.9	1.64	FM	SW	6.6	40, 80, 120	20
Adams (2000)*	15 M	22.3	1.94	FM	SW	6.6	FA	20
	15 F	22.5	1.61	FM	SW	6.6	120	17, 20, 23
Adams (2003a, 2003b)*	15 M	22.3	1.94	CH	SW	6.6	FA, 80	20
	15 F	21.4	1.65	CH	STEP	6.6	80	20
				FM	SW	6.6	FA, 80	20
				FM	STEP	6.6	80	20
Adams & Ollison (1997)*	12 M	23.5	1.98	FM	SW	6.6	FA, 120	17
				FM	RAMP	6.6	120, 120	17
Schelegle et al. (2009)*	16 M	21.4	2.04	CH	SW	6.6	FA	20
	15 F	21.4	1.73	CH	STEP	6.6	60, 70,	20
				CH	STEP	6.6	80, 87	20
McDonnell et al. (1991)*	38 M	24.7	2.01	CH	SW	6.6	FA, 80	20
	10 M	25.2	1.99	CH	SW	6.6	FA, 80, 100	20
McDonnell et al. (1983)	20 M	22.5	_	CH	SW	2.5	FA	35
	22 M	22.3	_	CH	SW	2.5	120	35
	20 M	23.3	_	CH	SW	2.5	180	35
	21 M	22.9	_	CH	SW	2.5	240	35
	21 M	23.1	_	CH	SW	2.5	300	35
	29 M	22.8	_	CH	SW	2.5	400	35
Koren et al. (1989)	11 M	25.4	_	CH	SW	2.0	FA, 400	35
Seal et al. (1993)	17M	26.8	1.94	CH	SW	2.33	FA	25
	15M	23.2	1.95	CH	SW	2.33	120	25
	15M	25.3	1.94	CH	SW	2.33	180	25
	16M	25.5	1.91	CH	SW	2.33	240	25
	15M	24.9	1.95	CH	SW	2.33	300	25
	15M	26.0	1.88	CH	SW	2.33	400	25
Kehrl et al. (1987)	8 M	20–30	_	CH	SW	2.25	FA, 400	35
Horstman et al. (1995)*	13 M	18–35	_	CH	SW	7.6	FA, 160	15
Folinsbee et al. (1988)*	10 M	25.3	1.94	CH	SW	6.6	FA, 120	20
Horstman et al. (1990)*	22 M	18–35	_	CH	SW	6.6	FA, 80, 100, 120	20
McDonnell et al. (1987)	26 M	18–30	_	CH	SW	2.0	FA, 180	35
McDonnell (1989)*	10 M	18–30	_	CH	SW	2.0	FA	35
	56 M	18–30	_	CH	SW	2.0	180	35

n, number of subjects; BSA, body surface area; M, male; F, female; CH, chamber exposure; FM, facemask exposure; SW, square wave concentration profile; RAMP, ramp concentration profile; STEP, stepwise concentration profile; FA, filtered air, V_E, minute ventilation.
*Indicate studies used to derive individual subject model coefficients. Unmarked studies were subsequently used to further validate the model.

intermittent exercise protocol (EVR = 35 L/min/BSA) 41 subjects were exposed to 0 (n = 13), 120 (n = 15) or 400 (n = 13) ppb O_3 for 2.5 h. The studies conducted in the EPA exposure chambers were approved by the Committee for the Protection of the Rights of Human Subjects of the University of North Carolina School of Medicine. The studies conducted in the University of California, Davis Human Performance Laboratory exposure facilities were approved by the Institutional Human Subjects Review Board of the University of California, Davis, CA, USA. All 704 subjects read and signed an approved statement of informed consent. Subjects were healthy, non-smoking, males (n = 628) or females (n = 76), 18–35 years of age. The number of subjects, gender, mean age, mean body surface area (BSA), and the exposure type, pattern, duration, mean O_3 concentration and target minute ventilation per BSA for each study used are given in Table 1. Data derived from O_3 exposure protocols and used for model fit and validation were corrected for filtered air responses by subtracting the filtered air values from the O_3 values at each measurement time point.

Statistical procedures and modeling

In order to estimate the dose of ozone at onset of FEV_1 response (Dos) and examine the subsequent development and recovery of FEV_1 decrements for individual subjects, a two compartment model with elements consistent with our previous analysis of the kinetics of O_3-induced tachypnea (Schelegle et al., 2007) was fit to FEV_1 measurements (Figure 1, Equations 1–4). Instantaneous inhaled O_3 dose rate (DR(t); μg/min), the input to compartment 1, triggers a step response once the cumulative dose of ozone (CD) reaches a threshold (Figure 1, Equation 1).

$$\mathrm{UOS}(t)=\frac{\mathrm{DR}(t)}{\left(1+\exp\left(-20\left(t-\left(\mathrm{Dos}\times t/\mathrm{CD}\right)\right)\right)\right)} \quad (1)$$

$$\mathrm{DR}(t)=[\mathrm{O_3}]\times V_\mathrm{E}\times 1.96 \quad (1a)$$

$$\mathrm{CD}=\int \mathrm{DR}(t)\,dt \quad (1b)$$

Uncompensated oxidant stress (UOS) enters compartment 2 at the rate it is produced in compartment 1 (UOS(t)) triggering the production of X at a rate proportional to UOS(t) (Figure 1). X is eliminated from the airway at a rate determined by the rate constant K_{el}. If UOS(t) is constant over time then X reaches a steady state (X_{SS} = UOS(t)/K_{el}) proportional to the rate of UOS(t) production (Equation 2). In order to accommodate for changes in DR(t), and as a result changes in UOS(t), the minute-by-minute change in X (ΔX) was calculated in an iterative fashion with X at beginning of a protocol being 0 (Equation 2a). The minute-by-minute (ΔX were then summed to obtain the amount of X contained in compartment 2 at each minute of the protocol (Equation 2a).

$$\Delta X=\left(\left(\frac{\mathrm{UOS}(t)}{K_{el}}\right)-X_{t-1}\right)\left(1-\exp(-K_{el})\right) \quad (2)$$

$$X_t=\sum \Delta X \quad (2a)$$

The percent change in FEV_1 is proportional to amount of X contained in compartment 2 with the proportionality constant (A) being an index of the responsiveness of the subject's FEV_1 response (Equation 3).

$$\%\mathrm{d}(\mathrm{FEV_1})=A\times X \quad (3)$$

The three model coefficients (Dos, K_{el} and A) were identified through minimization of the sum of squares error between the measured and modeled values. Particle Swarm Optimization identified the "global" minimum (Birge, 2003). The bounds for the candidate coefficients were fixed at the same values for all fittings and were estimated from the range of FEV_1 decrements observed for all the subjects in the data set. A population of random guesses at the problem solution, within the bounds, was initialized. These candidate solutions were improved through an iterative process. This was followed by nonlinear least squares curve fitting to better identify the local minimum. Once a candidate "global" minimum was reached, a new population of random guesses, which included the "global" best solution, was initialized, and the iterative process was repeated. This procedure was repeated several times to confirm that the solution had converged to the "global" minimum. In studies where resting V_E was not measured, a mean equivalent ventilation rate (EVR) of 7.82 L/min/m^2 derived from the Adams data (Adams, 2000a,2000b, 2002,

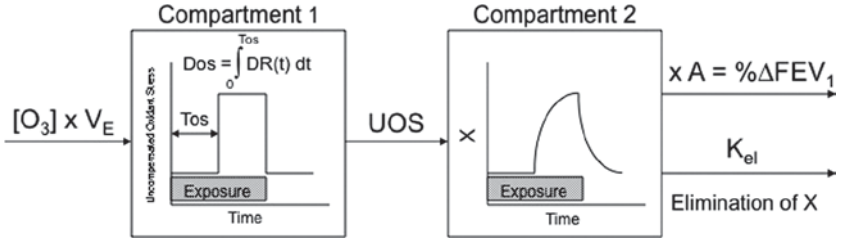

Figure 1. Diagram depicting a two compartment model for predicting the relationship between the inhaled dose rate (DR(t)) of ozone and the magnitude of decrements in forced expiratory volume in one second (FEV_1). The first compartment of this model consists of a delay function where Tos is the time to onset of response, while the second consists of an exponential growth and decay function. The model contains three coefficients. The first is the inhaled cumulative dose of ozone at the onset (Dos) of FEV_1 response or Tos. The second is the rate constant (K_{el}) for the elimination of an active substance, X that activates airway nerves and is produced at a rate proportional to the uncompensated oxidant stress (UOS) in compartment 1. The third is a proportionality coefficient (A) that relates the level of the X in compartment 2 to the individual subject's FEV_1 response.

2003a, 2003b, 2006a, and 2006b) for 102 subjects (57 males and 45 females) was used in combination with subject BSA to estimate resting V_E.

Measurements used for model fit and exclusion criteria

As the first goal of this study was to fit the proposed model to individual subject exposure–response, measurements derived from ozone inhalation studies in which FEV_1 was measured at least five times during exposure and recovery in at least one exposure protocol were selected. Using this criterion, the model was fit to the measurements from 301 subjects, from 14 studies containing 72 protocols (25 filtered air and 47 O_3 exposure protocols) (Table 1). After examining the distribution of the model parameters, an additional exclusion criterion was applied to the data set. If a subject's FEV_1 measurements contained a large offset, defined as an abrupt change in FEV_1 in either direction in the first sampling period that was maintained for several measurement periods afterward, then that subject's measurements were excluded from further analysis. These offsets were present in all the studies used and appear to be the result of the inherent variability of doing repeated FEV_1 measurements in certain subjects as they were present in both filtered air and O_3 protocols. Large offsets of this type were present in the data of 81 of the 301 subjects in the dataset. After applying this additional exclusion criteria 220 subjects remained (Table 2). Their model fits were included in a matrix (220 estimates of A, Dos and K_{el} plus each subjects anthropometric data) used to examine associations between the model coefficient estimates and subject anthropometric measurements and to predict the mean and variance of population responses.

Parameter distribution and correlation analysis

The distribution of coefficients estimates were examined using frequency distribution plots (Figure 3) and their fit to 57 possible distributions was examined (EasyFitXL, MathWave Technologies, Dnepropetrovsk, Ukraine). Best fit was determined using the Kolmogorov–Smirnov and Anderson–Darling criteria (EasyFitXL, MathWave Technologies). The association between the parameter estimates and subject anthrometric measurements (Table 1) were initially examined using bivariate Pearson correlation and subsequently analyzed using step-wise linear regression (SPSS, IBM Inc., Armonk, New York, USA).

FEV_1 variability

The variability in FEV_1 measurement was examined across and within protocols. The across protocol analysis was done using preexposure measurements. The within protocol analysis was done using the same approach used to examine FEV_1 responses within a O_3 exposure protocol where a percent change from baseline was calculated at each measurement time point.

Table 2. Subject physical characteristics and baseline pulmonary function measures that were collected from the 220 subjects (14 studies) whose FEV1 measures were used to develop the model.

	Gender	n	Mean	SD
Age (years)	M	169	24.1	3.9
	F	51	21.9	2.0
Height (cm)	M	169	180.0	7.9
	F	51	167.4	7.0
BSA (m^2)	M	169	1.96	0.17
	F	51	1.68	0.15
BMI, Wt (kg)/[Ht (m)]^2	M	169	23.7	2.8
	F	51	21.9	2.1
Body weight (kg)	M	169	77.1	11.1
	F	51	61.6	9.0
V_E (L/min)	M	169	39.3	13.4
	F	51	34.4	3.3
EVR (L/min/BSA)	M	169	20.4	7.1
	F	51	20.3	1.7
FEV_1 (L)	M	169	4.51	0.65
	F	51	3.46	0.44
A (%change FEV_1/μg O3/min)	M	169	−0.0201	0.0207
	F	51	−0.0208	0.0158
DOS (μg O_3)	M	134	1104	704
	F	47	1001	553
K_{el} (min^{-1})	M	134	0.0289	0.0385
	F	47	0.0127	0.0165

Values are mean (SD).

BMI, body mass index; BSA, body surface area; EVR, equivalent ventilation rate; FVC, forced vital capacity; FEV_1, forced expiratory volume in one second; MMEF, mid-maximal expiratory flow; PEF, peak expiratory flow; V_E, minute ventilation.

Validation

The 220 subjects' model coefficient estimates and BSA values were used to predict FEV_1 responses for all 62 O_3 exposure protocols in the dataset. The input to the model for each subject, DR(t), was calculated from Equation 1a, where V_E was estimated from the subject's BSA and the protocol target EVR. The estimated decrements in FEV_1 for each of the 220 subjects at each measurement time in each protocol were generated using Equations 1–3 with each subjects model coefficients (A, Dos, K_{el}) and the estimated DR(t) for each subject in each protocol as input. This initial step generated 220 values of predicted FEV_1 decrements (one for each subject) for each measurement time point contained in the 62 protocols (379 time points).

The ability to predict group mean responses using this approach was cross validated in two ways. Initially the 220 subjects' estimated decrements in FEV_1 for the 47 O_3 exposure protocols from the 14 studies used in the initial model fit were used for cross validation. If a subject participated in a given study/protocol their predicted FEV_1 decrements for that study/protocol were excluded from the matrix of predicted FEV_1 decrements. The mean predicted FEV_1 decrement for each time point was then calculated using the modified matrix. Linear regression of the observed mean for all subjects (n = 301) including those excluded from individual model fit versus the

average of the predictions was performed to examine the reliability and validity of the modeling approach. Second, additional cross validation was obtained by expanding the number of predicted decrements in FEV_1 to include the 15 protocols not used in the initial model fit. An additional, 484 subjects participated in one of these 15 protocols (number of subjects per exposure protocol varied from 12 to 52). Linear regression of the observed mean for all subjects in the dataset (n = 704) versus the average of the predictions revealed the accuracy of the model predictions (SPSS, IBM inc).

In order to determine whether there was a significant difference in variances and means of the FEV_1 responses obtained for each of the 62 exposure protocols used in the validation process, predicted and measured data for each time-point within each protocol were compared using Levene's test of equality of variance and Student t-test (SPSS, IBM Inc.). Levene's test is an inferential statistic used to assess the equality of variance in different samples and tests the null hypothesis that the population variances are equal. If Levene's test indicated the predicted and actual data did not have equal variance a t-test for unequal variance was used. Significance was set at a p value of 0.05 and adjusted using Holm's procedure for multiple comparisons within each protocol (Glantz, 2002). In order to examine the contribution of the inherent variability in repeated FEV_1 measurements in determining the variance at each sample period within a protocol, random changes in FEV_1 were assumed to be normally distributed and modeled using the standard deviation for percent change in FEV_1 during filtered air protocols for each subject (Excel, Microsoft Inc). The generated random percent changes in FEV_1 were then added to the predicted O_3-induced changes and again analyzed using Levene's test of equality of variance and Student t-test (SPSS, IBM Inc.).

Results

Subjects

Measurements from the 169 males and the 51 females were combined to develop and validate the two compartment model. The individual FEV_1 data of 220 subjects were fit to a two compartment model with DR(t) as input. Mean anthropometric data and estimated model parameters for the male and female subjects in the final data set are given in Table 2. There were significant differences between males and females for age, height, body surface area (BSA), body mass index (BMI), V_E and baseline FEV_1 (Table 2). There were no significant gender differences for the model estimates of Dos and A. K_{el} was significantly greater in males compared to females (0.029 ± 0.038 vs. 0.013 ± 0.017, p = 0.006). Data from both sexes were combined for all subsequent analysis.

Validation

Overall the individual subject measured and modeled FEV_1 decrements were highly correlated (mean R^2 of 0.69 ± 0.24). Forty-three subjects' data resulted in correlation coefficients (R) less than 0.40; 55 subjects had R values between 0.40 and 0.69; 78 subjects had R values between 0.70 and 0.89; and 44 subjects had R values between 0.90 and 1.00. The predictions of the mean decrements in FEV_1 for each study result in R values ranging from 0.79 to 0.98. The R for individual subject fits was greatest in those subjects that had the largest decrements in FEV_1 with O_3 exposure.

Comparison of all measured to all modeled FEV_1 decrements from the 220 subjects (1449 comparisons) yielded an R^2 = 0.640, a slope of 0.924 ± 0.008, and an intercept of 0.233 ± 0.061 (Figure 2A). The confidence intervals around the predicted versus the observed values regression line (Figure 2A) were small indicating a high reliability of the individual estimates.

The best fit line for the cross validation scatter plot of predicted versus actual mean FEV_1 decrement has a slope of 1.012 ± 0.027 and intercept is 0.093 ± 0.125 (Figure 2B). R^2 for the line fit to the cross validation scatter plot is 0.811 and was not significantly different from the line of identity. Comparison of the mean actual FEV_1 decrements versus the mean predicted FEV_1 decrements for all of the O_3 exposure protocols resulted in an R^2 = 0.819 with a best fit line slope of 0.957 ± 0.023 and an intercept of 0.233 ± 0.120 that was not significantly different from the line of identity (Figure 2C) supporting the validity of our modeling approach. For both of these regressions the confidence intervals around the mean predicted versus the mean observed values regression lines (Figure 2B and 2C) were small indicating a high reliability of the mean estimates.

Of the 379 measurement times contained in the entire data set (62 O_3 exposure protocols) there were 17 instances where the mean predicted and mean actual FEV_1 decrements were significantly different ($p \leq 0.05$). Each of these significant differences is indicated by arrows in Figures 4–6. Seven of these significant differences occurred in short duration protocols with five occurring in intermittent protocols involving an EVR of 35 L/min/m^2, where the predicted value was greater than the actual (Figure 4C). The remaining two of these seven significant differences occurred in protocols involving an EVR of 25 or 17 L/min/m^2, where the predicted value was less than the actual (Figure 4B). Five of these significant differences occurred in resting protocols of short (Figure 4A) or long duration (Figure 5A) where the predicted value was greater than the actual. One of the significant differences occurred at the fourth hour of an 8 h protocol with variable O_3 concentration averaging 120 ppb (Figure 6B). The remaining five significant differences occurred during recovery (two protocols; Figure 6A) or at the last measurement time of three protocols (Figure 5B and 5C) where the predicted values were less than the actual.

Comparison of variances of the predicted and actual FEV_1 decrements at each time point within each protocol resulted in a consistent pattern for 53 of the 62 protocols, with earlier time points having significantly different

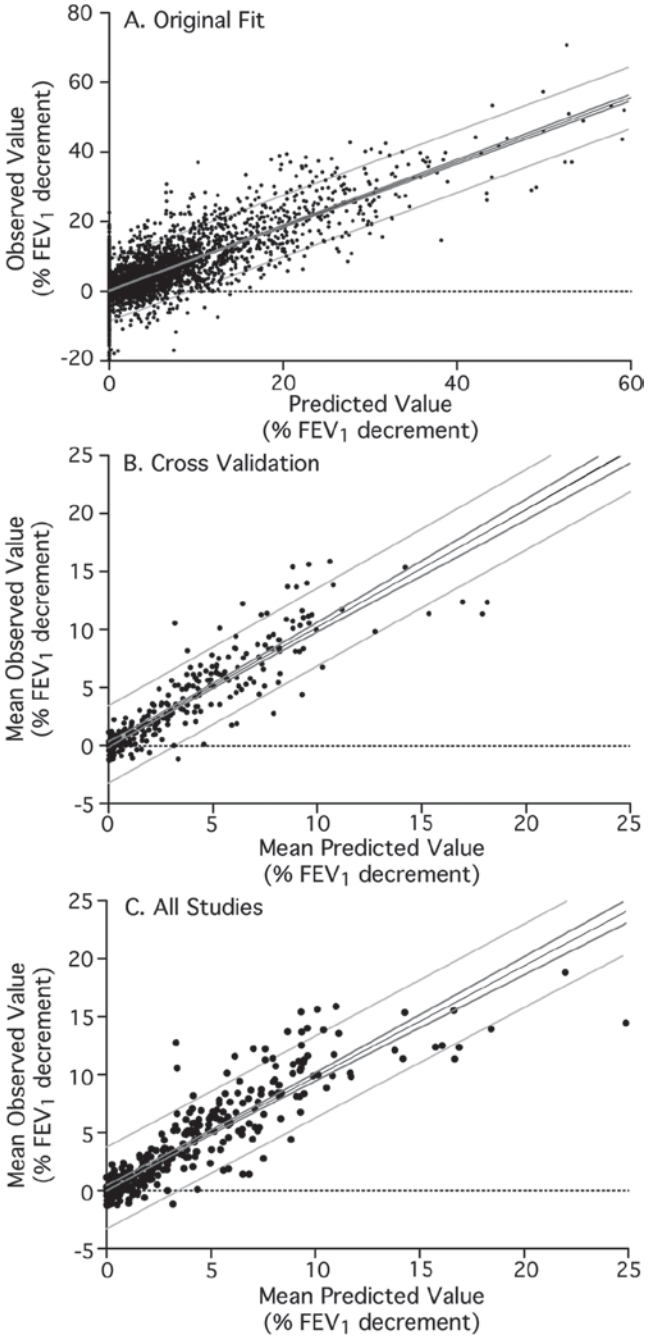

Figure 2. Scatter plots of observed versus predicted decrements in forced expiratory volume in one second (FEV_1). (A) Plot of individual subject's measured decrements in FEV_1 versus the predicted decrements in FEV_1 obtained during the original fit to the model. (B) Mean measured decrements in FEV_1 versus the mean predicted decrements in FEV_1 used for cross validation of the model. (C) Mean measured decrements in FEV_1 versus the mean predicted decrements in FEV_1 for all 21 studies used in the final validation of the model. The inner dark gray lines are the 95% confidence bands for the regression. The outer light gray lines are the 95% predictive bands for the regression and indicates the region in which 95% of future data will lie.

variances. The difference in variances was maintained until the mean predicted FEV_1 decrement exceeded 3.53 ± 2.26 or 54.0 ± 11.2% of the subjects mean predicted FEV_1 decrement was greater than 0. The extreme of this pattern was observed in eight protocols where the variance was significantly different for the entire protocol. The mean maximum predicted FEV_1 decrement attained in these protocols was 2.66 ± 2.33%. In the remaining nine protocols the variance at early time points of the predicted and actual FEV_1 decrement data was not significantly different. These nine protocols were short duration protocols (1–2.5 h) with an exercise EVR of 25 L/min/m² or greater and exposure to 240 ppb O_3 or greater where the mean predicted FEV_1 decrement was 7.49 ± 3.79 and 61.9 ± 12.3% of the subjects mean predicted FEV_1 decrement was greater than 0. Adding random percent changes in FEV_1 to the predicted O_3-induced changes reduced the number of protocols with early time points having significantly different variances from 53 to 14. Protocols where early significant differences in variance persisted were characterized by greater standard deviations than the predicted. These larger standard deviations were due to the subset of subjects previously identified to have an early offset in their FEV_1 data. This analysis demonstrates that a relatively small mean predicted FEV_1 decrement needs to be generated in order to reach a point where there is no longer any significant difference in variance between predicted and actual values and that in the majority of cases differences in variances can be accounted for by adding random percent changes in FEV_1 approximating the variance observed in filtered air protocols to the predicted O_3-induced changes.

Distribution of model parameters

The frequency distribution of the model estimates of Dos, K_{el} and A are shown in Figure 3A–C. The histogram of the estimated proportionality constant, A, includes the values for all 220 subjects. The histograms of the estimates of Dos and K_{el} include estimates from 181 subjects. Estimates of Dos and K_{el} were excluded from these histograms ($n = 39$) if the estimated proportionality constant, A, was less than 10^{-5} and/or the estimated Dos was greater than 2500 μg and greater than 90% of the subjects maximum cumulative dose of ozone greatly reducing the reliability of the estimated values of Dos and K_{el} for these subjects. None of the three estimated parameters are normally distributed. Dos fits an inverse gaussian distribution with a mean of 1078 ± 668 μg O_3. K_{el} fits a lognormal distribution with a mean of 0.0289 ± 0.055 s^{-1}. The proportionality constant, A, fits a generalized pareto distribution with a mean of 0.0203 ± 0.0197% change in FEV_1/μg O_3.

Among the 181 subjects for which there were reliable estimates of Dos, K_{el} and A there were significant correlations between the estimates of Dos and K_{el}, and subject anthropometric and exposure parameters. The estimates of Dos were slightly, but significantly correlated with age (R = 0.212, p = 0.004), protocol EVR (R = –0.159, p = 0.032) and baseline FEV_1 (R = 0.146, p = 0.050). The estimates of K_{el} were significantly correlated with age (R = 0.186, p = 0.012), height (R = 0.163, p = 0.028), and baseline FEV_1 (R = 0.251, p = 0.001). There were no significant

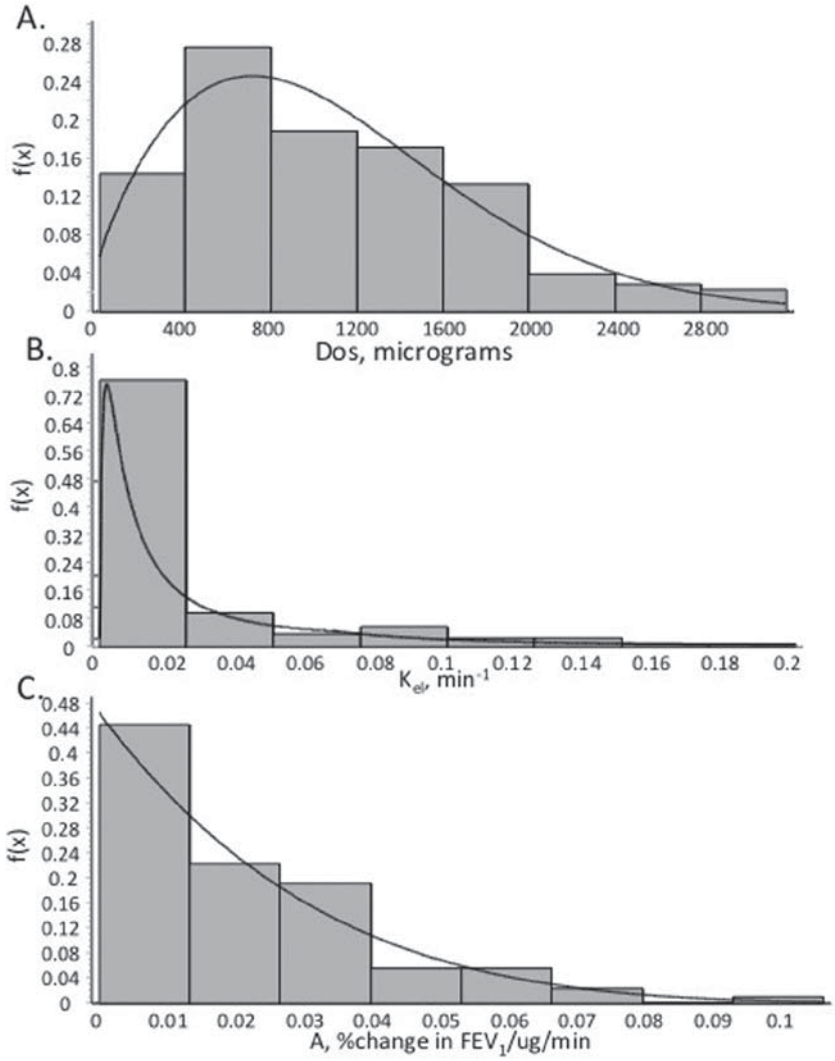

Figure 3. Probability distribution histograms and the fitted probability distribution curves (solid lines) for (A) Dos, (B) rate constant (K_{el}) and (C) proportionality coefficient (A).

correlations between the estimated proportionality coefficient, A, and any of the subject anthropometric or exposure parameters. This analysis implies that while anthropometric parameters weakly influence the kinetics of the ozone-induced FEV_1 response, they do not influence the proportionality coefficient, A, that determines maximal FEV_1 response at any dose rate.

Stepwise linear regression indicated that Dos is best predicted by age alone (Equation 4; $R^2 = 0.040$, $p = 0.004$), while, K_{el} is best predicted by age in combination with baseline FEV_1 (Equation 5; $R^2 = 0.085$, $p = 0.001$).

$$\text{Dos} = 156.4\ (\pm 321.2) + 39.4\ (\pm 13.6)\ \text{Age} \quad (4)$$

$$K_{el} = -0.063\ (\pm 0.021) + 0.002\ (\pm 0.001)\ \text{Age} + 0.011\ (\pm 0.003)\ \text{baseline FEV}_1 \quad (5)$$

The estimated model coefficients, Dos, K_{el} and A were all significantly correlated with each other. There was a slight to low correlation between Dos and K_{el} ($R^2 = 0.034$, $p = 0.013$), and Dos and A ($R^2 = 0.077$, $p < 0.001$), while, K_{el} was moderately correlated with A ($R^2 = 0.309$, $p < 0.001$).

Prediction of population responses

Our modeling approach reliably predicted the mean FEV_1 decrements for 704 subjects who participated in 76 O_3 exposure protocols. In addition, the predicted versus measured regression using all protocols and subjects indicates that the 220 subjects are representative of the remaining 484 subjects in the data set. Plots of the observed mean values of percent change in FEV_1 and predicted mean values of percent change in FEV_1 for short (Figure 4A–C) and prolonged (Figure 5A–C) duration constant O_3 exposure protocols indicate that the model estimates describe the measured mean FEV_1 response well for the range of exposure protocols included in the data set. Similar plots for protocols using variable O_3 concentration and V_E are shown in Figure 6A–C. An exception was that estimated model parameters of 11 subjects resulted in extremely high predicted decrements in FEV_1, in excess of the maximum measured FEV_1 decrement

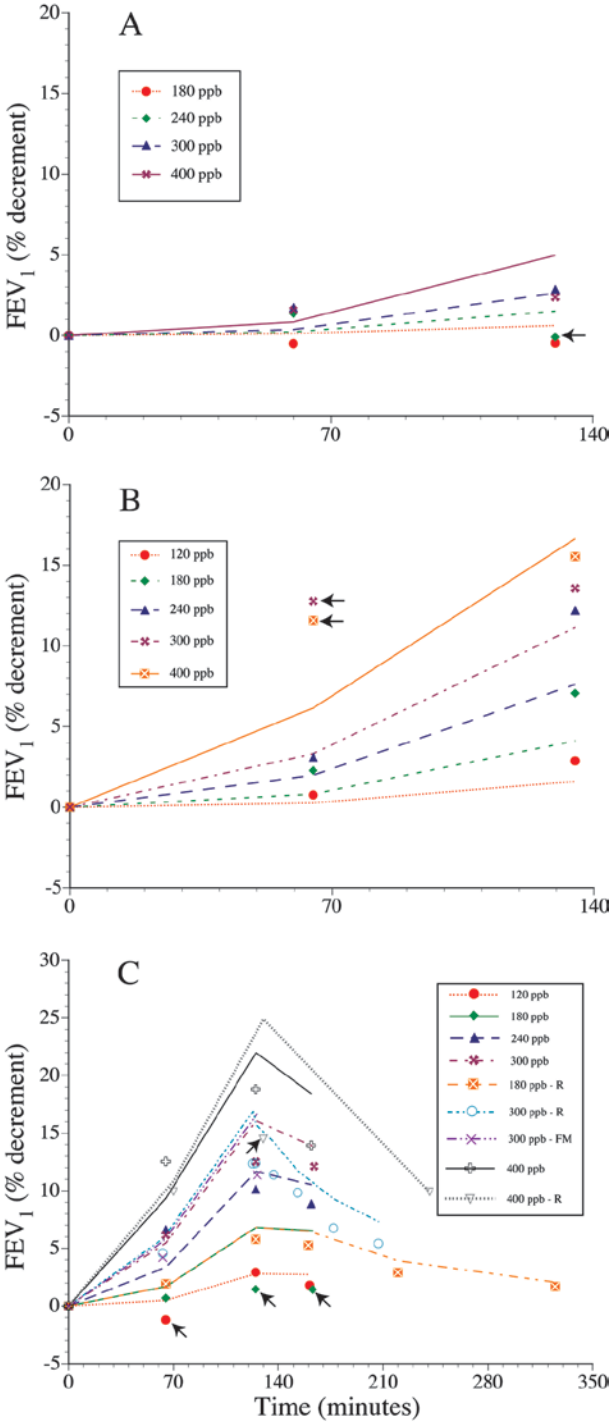

Figure 4. Mean observed decrements in forced expiratory volume in one second (FEV_1) (symbols) and mean predicted decrements in FEV_1 (lines) for 2–2.5 h O_3 exposure protocols at rest (A) or with intermittent exercise where minute ventilation was set at an equivalent ventilation rate (EVR) of 20 L/min/BSA (B) or 35 L/min/BSA where symbols beyond 150 min represent measured recovery (R) FEV_1 values post exposure at rest (C). Arrows indicate observed values that were significantly different ($p < 0.05$) from predicted values.

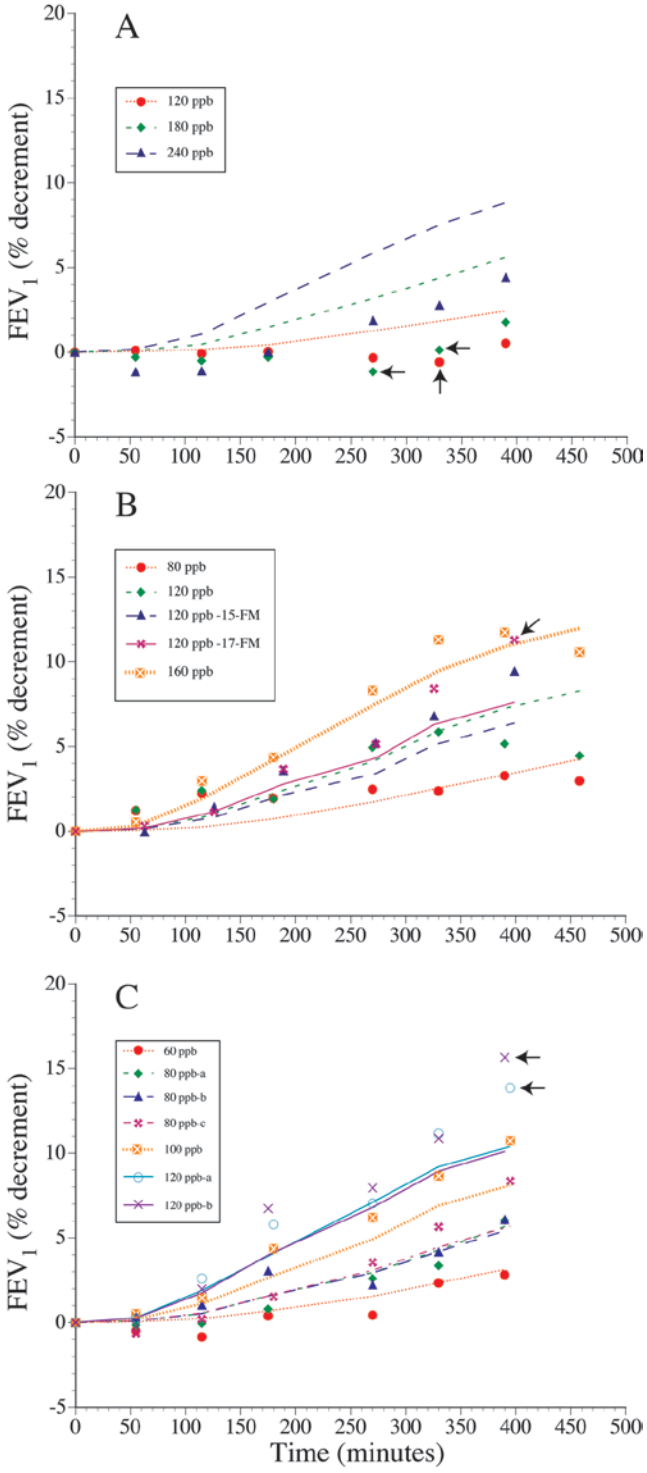

Figure 5. Mean observed decrements in FEV_1 (symbols) and mean predicted decrements in FEV_1 (lines) for 6.6–7.6 h O_3 exposure protocols at rest (A) or with quasi-continuous exercise where minute ventilation was set at an equivalent ventilation rate (EVR) of 15 and 17 L/min/BSA (B) or 20 L/min/BSA (C). Arrows indicate observed values that were significantly different ($p < 0.05$) from predicted values.

contained in the data set, for the short-duration protocols (2.5 h) involving heavy exercise (EVR = 35 L/min/BSA) and high ozone concentrations (240, 300 and 400 ppb). We speculate that these subjects could represent the small number of subjects who were fit enough to complete these heavy exercise regimens but would have chosen not to perform such exposure protocols or would have chosen to voluntarily terminate exposure once begun. Given this possibility predicted FEV_1 decrements

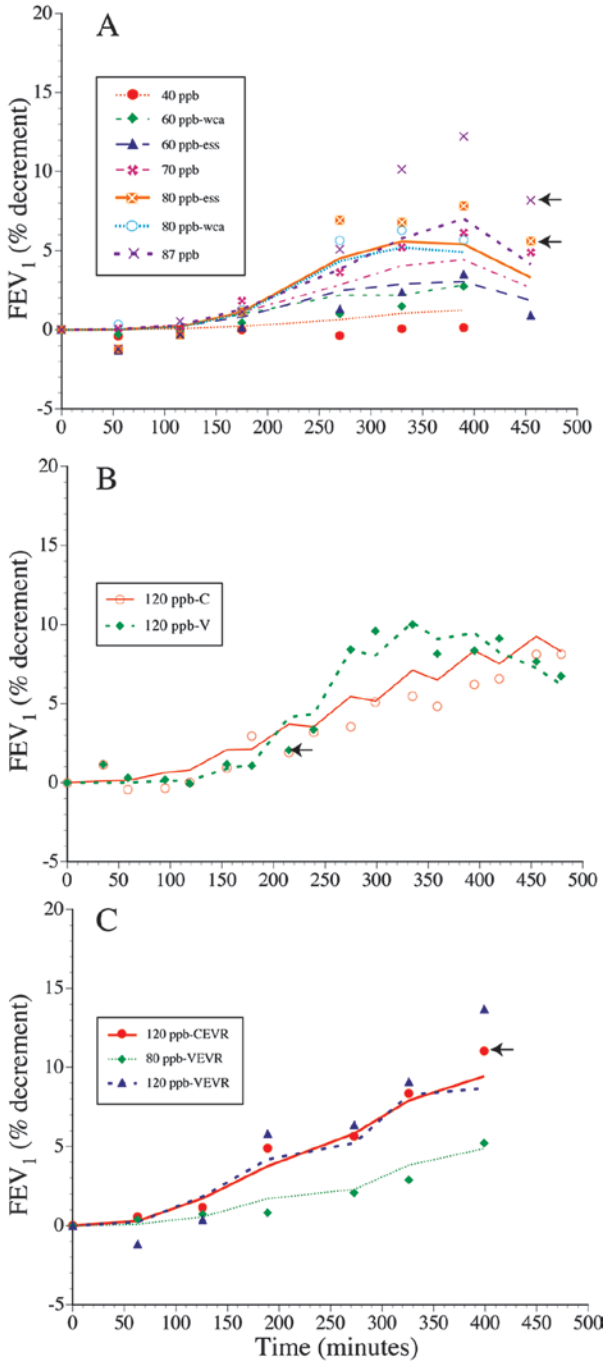

Figure 6. Mean observed decrements in forced expiratory volume in one second (FEV_1) (symbols) and mean predicted decrements in FEV_1 (lines) for: (A) 6.6 h O_3 exposure protocols (7.6 h FEV_1 values post exposure at rest) with quasi-continuous exercise where minute ventilation was set at an equivalent ventilation rate (EVR) of 20 L/min/BSA and O_3 concentration was varied in a stepwise fashion with common Adams 2006a (WCA) and Schelegle et al. 2009 (ESS) exposures differentiated; (B) 8 h O_3 exposure protocols with intermittent exercise where minute ventilation was set at an EVR of 20 L/min/BSA and O_3 concentration was held constant (ppb-C) or varied (ppb-V) in a stepwise fashion; or (C) 6.6 h O_3 exposure protocols with quasi-continuous exercise where minute ventilation was constant at an EVR of 15 L/min/BSA (CEVR) or varied (VEVR) and O_3 concentration was held constant. Arrows indicate observed values that were significantly different ($p < 0.05$) from predicted values.

greater than 70 percent were removed from the Figure 4C data set. In contrast, for prolonged duration protocols, involving both constant and variable O_3 concentrations, the predicted individual subject FEV_1 decrements were all less than 70% and were within the range observed in the actual data.

The development of a progressively skewed distribution of FEV_1 decrements with time and the contributions of the three model coefficients during the 8 hour prolonged duration protocols (EVR = 20, constant 120 ppb O_3) of Adams (2006b) is illustrated in Figure 7. At each of the 2 h time points more subjects are predicted to have decrements in FEV_1. These decrements in FEV_1 are predicted to occur in the individuals who have Dos that is in the lower quartile. Once Dos is reached the magnitude of the predicted FEV_1 decrement is the result of the interaction between K_{el} and A, where a moderately low K_{el} in combination with moderately high A results in the greatest predicted FEV_1 decrements. Disregarding the intrasubject sources of variability that are evident in the observed data the model appears to describe an increasing variability as a skewed response with increasing exposure that is generally consistent with observed data.

Discussion

Dos quantifies the delay to the onset of response as a function of the accumulating inhaled dose of O_3 during exposure. The Dos was first quantified by Schelegle et al. (2007) using breathing pattern data and later using FEV_1 data obtained during prolonged exposure (Schelegle et al., 2009). Dos is a distinct individual characteristic that is independent of the magnitude of ozone-induced response and is not influenced by changing ozone concentration and only mildly influenced by changing V_E (Schelegle et al., 2007, 2009). The mean estimated Dos of 1078 ± 668 μg O_3 in the current analysis is similar to previously derived values (Schelegle et al., 2007) and was shown to fit a skewed inverse gaussian distribution. Dos was found to correlate with age and EVR and to be best predicted by age alone, however, given an R^2 of 0.040, age accounts for only a small fraction of the variance in Dos. The underlying mechanisms that result in Dos have not been identified. One plausible hypothesis would postulate one or more antioxidant systems that need to be reduced within the airway lining fluid and/or within airway epithelial cells before O_3 can produce reaction products acting on epithelial cells to release arachidonic acid that is then converted to prostinoids by cyclooxygenase. One or more of these prostinoids then activate bronchopulmonary C fibers that mediate the reflex decrements in pulmonary function and subjective symptoms that are characteristic of O_3 inhalation in humans (Schelegle et al., 2007). Once Dos is reached the rate at which cycloxygenase products are produced would be proportional to dose rate while their rate of metabolism and/or elimination would be described by the rate constant, K_{el}. The mean estimated K_{el} was –0.0289 ± 0.055 s^{-1} and fit a lognormal

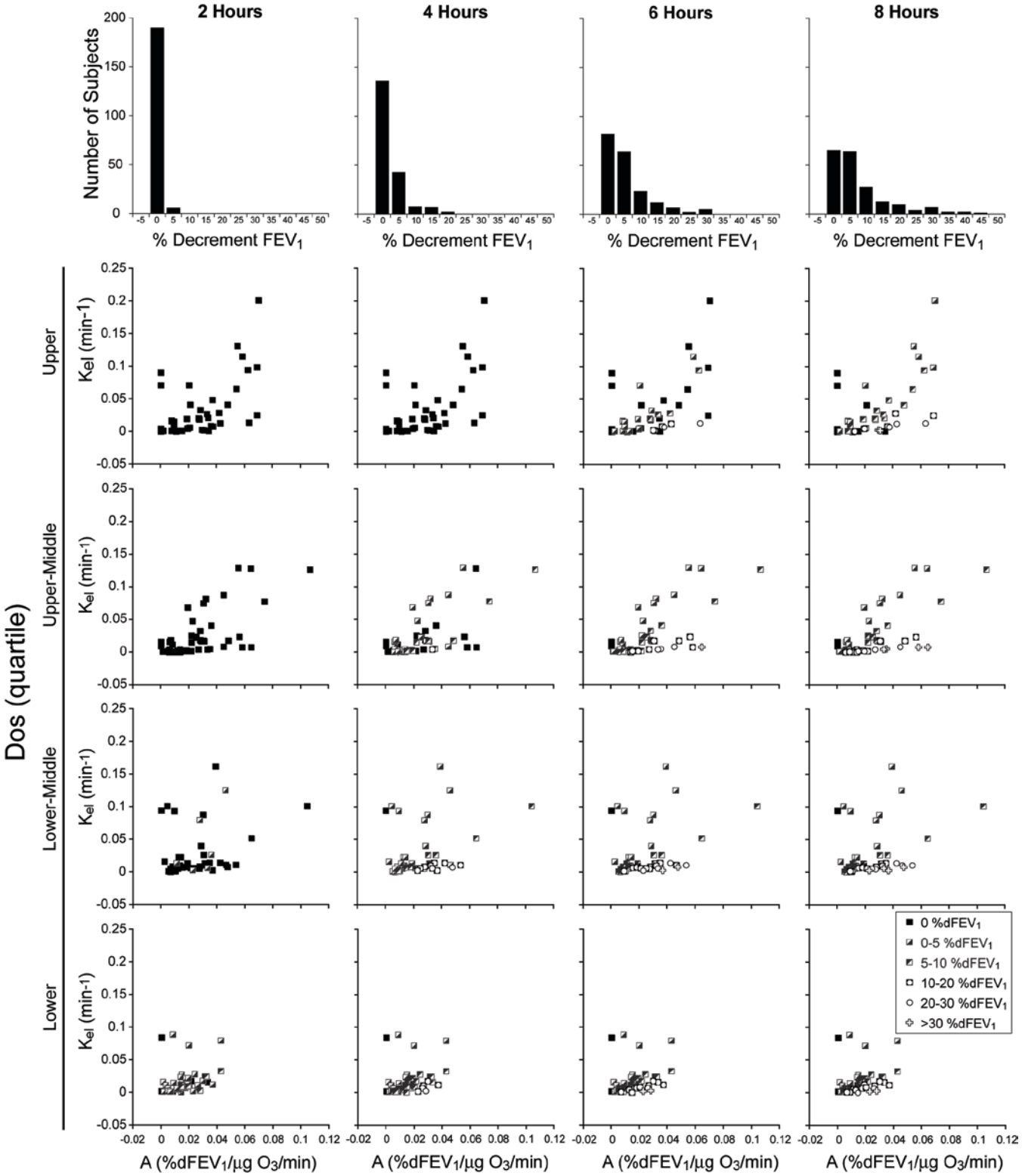

Figure 7. Role of model coefficients, Dos, K_{el} and A, in the development of a skewed distribution of predicted decrements in FEV_1 at 2 h intervals during an 8 h O_3 exposure protocol with intermittent exercise (EVR = 20 L/min/BSA) at constant O_3 concentration of 120 ppb where exercise was performed during the first half hour of every hour (Adams 2006b). The upper panels are subject frequency distribution histograms for predicted interval decrements in FEV_1. Scatter plots of K_{el} versus A are organized according to quartiles of Dos (rows) at 2 h intervals (columns). Magnitude of decrement in FEV_1 is indicated by different symbols.

distribution. K_{el} was found to be best predicted by age (R^2 = 0.035) and baseline FEV_1 (R^2 = 0.063). As with Dos, age and baseline FEV_1 account for only a small fraction of the variance in K_{el}. The magnitude of the proportionality coefficient, A, would then be determined by the amount of cyclooxygenase products present as determined by the interaction between their production and elimination and/or the degree of reflex gain/amplification that

leads to reduced lung volumes and decrements in FEV_1. The large variance in the individual estimates of A, Dos and K_{el} combined with weak association of these coefficicients with anthropometric characteristics supports the proposition that the major factors that drive the O_3-induced FEV_1 response are metabolic and neural. These metabolic and neural factors appear to be modified by age, BMI and baseline FEV_1, but these effects are small compared to the variance in the metabolic and neural mechanisms.

The approach used in this analysis has possible limitations related to the model and dataset used. The observation that the estimated model coefficients for 5% of the subject's results in extreme predicted FEV_1 decrements for protocols that combine severe exercise with high O_3 concentrations for short durations suggest that the model is limited. There are three possible explanations for these large predicted decrements in FEV_1. First, these large predicted decrements are real, the subjects for which these predicted large FEV_1 decrements were derived represent individuals knowing their sensitivity to air pollution would have chosen not to perform short-duration, heavy exercise, high O_3 concentration protocols or would have chosen to voluntarily terminate exposures once begun because of severe symptoms of discomfort. Second, it is possible that when symptoms become severe an as yet unkown process acts to limit symptoms and FEV_1 decrements. McDonnell et al. (1999) accounts for such a mechanism in their model. Third, the model coefficients derived for these individuals using primarily longer duration but lower concentration exposures could be further optimized by including responses to short duration, high concentration exposures in their dataset.

The proposed two compartment model is simple and may not describe FEV_1 decrements induced by a wide range of exposure conditions. However, there were only 17 time points out of 379 (4.5%) in the whole dataset where the mean observed FEV_1 response was significantly different from the predicted mean response. The regression of the mean predicted versus the mean observed decrements in FEV_1 for the dataset indicates that overall the model produced both valid and reliable mean estimates. This being said, the observed 17 significant difference between the mean predicted and mean observed values suggests that the model could be improved. One modification would be to adjust the model to account for the effect of variable minute ventilation on Dos. The observation of a significant negative correlation between Dos and EVR confirms the previous observation that Dos decreases as minute ventilation increases (Schelegle et al., 2007, 2009). Adjusting the model accordingly would reduce the estimated response in resting protocols (Figure 4A and 5A) and shorten time to onset of response in protocols involving moderate to severe exercise (Figure 4B and 4C). The other way to look at the 17 significant differences between observed and estimated FEV_1 values identified in Figures 4–6 is to consider the dataset. The data set is composed 379 observations from 62 exposure protocols with the number of subjects completing each protocol varying from 12 to 62. The degree to which the mean observed response generated from these protocols represent the "population mean" for healthy young adults from 18–35 years of age needs to be considered. Two examples stand out. In Schelegle et al. (2009) 8 of 31 subjects were very responsive to ozone and it was their marked responses that resulted in the marked differences seen in the 87 ppb exposure illustrated in Figure 6A. The second example is the two protocols combining short duration exposure (2 h) with severe exercise at 180 ppb (Figure 4C). In one of these protocols the observed response closely tracks the predicted response (180 ppb – R, in the figure legend), while in another the model significantly over predicts the observed response (180 ppb, in the figure legend).

The reliable modeling of individual responses requires sufficient information before and after the onset of response and therefore limits the studies in which the individual subject kinetics and responsiveness can be reliably determined. Another consideration in the modeling of individual ozone-induced FEV_1 responses is the inherent variability in the repeated measurement of FEV_1 on different days and within a single protocol. This inherent variability in the measurement of FEV_1 limits the ability to distinguish the onset of response, especially in subjects with low responsiveness and in extreme cases prevents the ability to obtain reliable estimates when individual subject's data contained large offsets. Accordingly, to reliably derive each of the three model coefficients individual subject's data were extracted from exposure response studies containing the minimum amount of data to fit the model and data from subjects (n = 81) that contained large offsets was excluded. The exclusion of these 81 subjects from the dataset used to derive the model coefficients raises the concern that our mean estimates of FEV_1 decrements are biased by excluding subjects with more reactive airways or other physiologic mechanisms. The cause or causes of the observed offsets could not be identified as they were observed in filtered air as well as ozone protocols, went in both directions, would be present on one day and not another, and were present in both responsive and non-responsive subjects. The only factor that appears to be associated with the presence of a large offset in a subject's data was a higher than average day-to-day variability in FEV_1 as determined by the standard deviation in their preexposure FEV_1.

While it was possible to fit individual data to the model, it is important to recognize that the entire data set was limited by the information available in each of the study designs. With the exception of two studies, McDonnell et al. (1987) and Adams (2003a), there is limited recovery response data following exposure reducing the ability to estimate K_{el}. McDonnell et al. (1987) studied 26 healthy asymptomatic male subjects with allergic rhinitis aged 18–35 years, who inhaled 180 ppb O_3 for 2.75 h while performing heavy intermittent exercise (EVR = 35 L/min/BSA)

followed by a 2.75 h recovery period during which FEV_1 was evaluated three times. The mean estimated K_{el} for this study was 0.0400 ± 0.0346 min^{-1} compared to a mean value of 0.0289 ± 0.055 s^{-1} for all the studies from which K_{el} was estimated. As a result the estimated mean half-time of recovery is longer for all the studies from which K_{el} was estimated (24.0 min) compared to the half-life of recovery estimated for subjects in McDonnell et al (1987) (17.3 min). While potentially improving the estimates of K_{el}, the estimates of Dos derived from McDonnell et al (1987) were limited by the number of measurements of FEV_1 during exposure, illustrating that a diverse study design will provide the best coefficient estimates. As discussed above, coefficient estimates derived from studies composed primarily of prolonged exposure protocols led to some predicted FEV_1 decrements for short-duration, heavy exercise, high O_3 concentration protocols that were extremely large and in excess of those observed in the actual data suggesting that the model may not always accurately predict responses at much higher exposures when model coefficients are derived using a limited dataset. The best study design for estimating individual subject model coefficients would be one that combines prolonged and short duration exposures with cumulative inhaled dose >3000 μg O_3 followed by multiple measurements of FEV_1 during and post exposure over a recovery period lasting 4–6 h. The study that was closest to using this design was Adams (2003a, 2003b).

The current analysis suggests that Dos, K_{el} and A interact to determine the magnitude of FEV_1 response in individual subjects and that this interaction leads to the development of a skewed O_3-induced FEV_1 population response. This interaction is illustrated in Figure 7 using data derived from Adams (2006b) where subjects completed an 8 h O_3 exposure protocol with intermittent exercise (EVR = 20 L/min/BSA) at constant O_3 concentration of 120 ppb with exercise during the first half hour of every hour. As the cumulative inhaled dose of O_3 increases the first subjects to exhibit decrements in FEV_1 would have a Dos in the lower quartile of its frequency distribution. The interaction between K_{el} and A at this point determines the rate at which FEV_1 decrements begin to develop with the rate of change being greatest when A is large and K_{el} is small. The result is that early in the exposure most individuals show no response. As the cumulative inhaled dose increases Dos is attained in a greater number of individuals and these individuals also begin to develop decrements in FEV_1 while the variance of the FEV_1 response transitions from being unequal to not being significantly different. As the cumulative dose exceeds the mean Dos (1078 μg) and approaches 2500 μg O_3 the majority of individuals develop FEV_1 decrements. If Dos is reached early enough and the exposure is of sufficient duration FEV_1 decrements will plateau with the magnitude of FEV_1 decrements at this plateau being determined by the values of K_{el} and A. The skewed O_3-induced FEV_1 response in a population is therefore the result of each individuals response function and the individual's maximum decrement that can be attained at a given dose rate, these variables being determined by the interaction of Dos, K_{el} and A.

Ideally a predictive model should account for the large variability observed in individual's O_3-induced responses (EPA, 1996). Similar to the fit of anthropometric parameters to model coefficients in the current analysis, age, BSA, or BMI account for only a small fraction of the variance in O_3-induced FEV_1 decrements in the models. The combination of fitting individual subject data to a simple exposure-response model and then creating a matrix from the derived model coefficients in the current analysis has the advantage that it retains more of the information related to variation in individual subject responsiveness and not just that small fraction of variance that is accounted for by one or two anthropometric parameters. On the other hand, this approach did not result in predictive model similar to McDonnell et al's (1997, 1999, 2007, 2010) where group mean responses are predicted using anthropometric parameters (age and BMI) as an input. In the current study the importance of age, and baseline FEV_1, but not BMI appears to affect the distributions of coefficients describing the kinetics of response (Dos and K_{el}). Substituting Dos and K_{el} with the regression equations describing their relationship with age and baseline FEV_1 into Equations 1–3 would result in a predictive model (Equations 6–8) that predicts mean response in groups that vary in these parameters, but no longer describes the distribution of response.

$$\mathrm{UOS}(t)=\frac{\mathrm{DR}(t)}{\left(1+\exp\left(-C_{os}\left(t-\left(\left(\beta_1+\beta_2(\mathrm{Age})\right)\times t/\mathrm{CD}\right)\right)\right)\right)} \quad (6)$$

$$X_t=\sum\left(\frac{\mathrm{UOS}(t)}{\left(\beta_3+\beta_4(\mathrm{Age})+\beta_5(\mathrm{bFEV}_1)\right)}-X_{t-1}\right)\times\left(1-\exp\left(-\left(\beta_3+\beta_4(\mathrm{Age})+\beta_5(\mathrm{bFEV}_1)\right)\right)\right) \quad (7)$$

$$\%\mathrm{dFEV}_1=A\times X_t \quad (8)$$

Where C_{os} is a coefficient describing the distribution of Dos in the population, while β_1, β_2, β_3, β_4 and β_5 are the regression coefficients relating age and baseline FEV_1 ($bFEV_1$) to Dos and K_{el}. The model coefficients (C_{os}, β_1, β_2, β_3, β_4 and β_5) would need to be further optimized using the whole dataset and techniques similar to McDonnell et al. (2007, 2010).

Conclusions

Exposure–response data derived from 21 studies conducted between 1980 and 2009 at the EPA exposure chambers on the University of North Carolina and the human exposure facilities in the Human Performance Laboratory on the University of California Davis were used to validate a two-compartment model of ozone-induced decrements in FEV_1. Three model coefficients Dos, K_{el} and A that describe the kinetics of O_3-induced

FEV_1 impairment were estimated using the exposure conditions (V_E, $[O_3]$, duration of exposure) of 220 individual subjects from 14 studies. The modeling approach used not only produces reliable estimates of group mean responses, but also reproduces the variance of response when the predicted FEV_1 decrement exceeds a minimal value. The generated matrix of model coefficients can be used to predict FEV_1 decrements in healthy individuals 18–35 years of age induced by a wide range of O_3 exposure conditions, including those not included in the data set. Though Dos and K_{el} were significantly correlated with age, age accounted for only a small fraction of the variance in these coefficients and therefore a small fraction of the variance in the predicted group mean decrements in FEV_1. Finally, examination of the matrix of predicted FEV_1 impairment confirms that the modeling approach used reproduces the skewed distribution of O_3-induced FEV_1 response observed in the O_3 exposure response literature and therefore preserves the large individual variability characteristic of O_3 response.

The modelling of individual subject data to generate a matrix of model coefficients that can be used to predict FEV_1 decrements induced by a wide range of O_3 exposure conditions represents a novel approach for evaluating the health risk associated with exposure to ambient O_3. Preserving the individual variability characteristic of O_3 response not only results in the ability to predict population mean responses but also the frequency distribution of the response as well. As such this approach provides a potential starting point for improving the risk assessment of environmental O_3 exposure that would include a coefficient describing the delay in response. In addition, the ability to better characterize a subject's responsiveness to ozone using Dos, K_{el} and A provides a useful tool to better understand the mechanisms leading to ozone-induced responses.

Acknowledgements

The authors thank William McDonnell for sharing the EPA data base with us and providing insights into his modelling this data set. The authors thank Will Olison and William McDonnell for reading an early version of the manuscript and providing their comments and insights.

Declaration of interest

This research was funded by an unrestricted gift from the American Petroleum Institute.

References

Adams WC. 2000a. Feasibility study of prolonged ozone inhalation exposure via face mask. Inhal Toxicol 12:299–313.

Adams WC. 2000b. Ozone dose-response effects of varied equivalent minute ventilation rates. J Expo Anal Environ Epidemiol 10:217–226.

Adams WC. 2002. Comparison of chamber and face-mask 6.6-hour exposures to ozone on pulmonary function and symptoms responses. Inhal Toxicol 14:745–764.

Adams WC. 2003a. Comparison of chamber and face mask 6.6-hour exposure to 0.08 ppm ozone via square-wave and triangular profiles on pulmonary responses. Inhal Toxicol 15:265–281.

Adams WC. 2003b. Relation of pulmonary responses induced by 6.6-h exposures to 0.08 ppm ozone and 2-h exposures to 0.30 ppm ozone via chamber and face-mask inhalation. Inhal Toxicol 15:745–759.

Adams WC. 2006a. Comparison of chamber 6.6-h exposures to 0.04-0.08 PPM ozone via square-wave and triangular profiles on pulmonary responses. Inhal Toxicol 18:127–136.

Adams WC. 2006b. Human pulmonary responses with 30-minute time intervals of exercise and rest when exposed for 8 hours to 0.12 ppm ozone via square-wave and acute triangular profiles. Inhal Toxicol 18:413–422.

Adams WC, Ollison WM. 1997. Effects of prolonged simulated ambient ozone dosing patterns on human pulmonary function and symptomatology. June 8–13, 97-MP9.02, pp. 1–16.

Adams WC, Savin WM, Christo AE. 1981. Detection of ozone toxicity during continuous exercise via the effective dose concept. J Appl Physiol 51:415–422.

Birge B. 2003 PSOt - a particle swarm optimization toolbox for use with Matlab. IEEE Swarm Intelligence Symposium. Indianapolis, Indiana, IEEE.

EPA (1996) Air quality criteria for ozone and related photochemical oxidants. In: Development OOR, ed. Research Triangle Park, NC: NTIS, Springfield, VA.

Folinsbee LJ, Drinkwater BL, Bedi JF, Horvath SM. 1978 The influence of exercise on the pulmonary function changes due to low concentrations of ozone. In: Folinsbee LJ, ed. Environmental Stress. New York: Academic Press.

Folinsbee LJ, McDonnell WF, Horstman DH. 1988. Pulmonary function and symptom responses after 6.6-hour exposure to 0.12 ppm ozone with moderate exercise. JAPCA 38:28–35.

Glantz SA 2002 Primer of biostatistics, New York: McGraw-Hill, Medical Pub. Div.

Hazucha M, Silverman F, Parent C, Field S, Bates DV. 1973. Pulmonary function in man after short-term exposure to ozone. Arch Environ Health 27:183–188.

Hazucha MJ. 1987. Relationship between ozone exposure and pulmonary function changes. J Appl Physiol 62:1671–1680.

Horstman DH, Ball BA, Brown J, Gerrity T, Folinsbee LJ. 1995. Comparison of pulmonary responses of asthmatic and nonasthmatic subjects performing light exercise while exposed to a low level of ozone. Toxicol Ind Health 11:369–385.

Horstman DH, Folinsbee LJ, Ives PJ, Abdul-Salaam S, McDonnell WF. 1990. Ozone concentration and pulmonary response relationships for 6.6-hour exposures with five hours of moderate exercise to 0.08, 0.10, and 0.12 ppm. Am Rev Respir Dis 142:1158–1163.

Kehrl HR, Vincent LM, Kowalsky RJ, Horstman DH, O'Neil JJ, McCartney WH, Bromberg PA. 1987. Ozone exposure increases respiratory epithelial permeability in humans. Am Rev Respir Dis 135:1124–1128.

Koren HS, Devlin RB, Graham, DE, Al E. 1989 Ozone-induced inflammation in the lower airway of human subjects. Am.Rev. Respir.Dis 139:407–415.

Kulle TJ, Sauder LR, Hebel JR, Chatham MD. 1985. Ozone response relationships in healthy nonsmokers. Am Rev Respir Dis 132:36–41.

Mcdonnell WF 1989 Individual variability in the magnitude of acute respiratory response to ozone exposure. In: Frank MJUAR, ed. Susceptibility to inhaled pollutants. Philadelphia:American Society for Testing and Materials.

McDonnell WF, Horstman DH, Abdul-Salaam S, Raggio LJ, Green JA. 1987. The respiratory responses of subjects with allergic rhinitis to ozone exposure and their relationship to nonspecific airway reactivity. Toxicol Ind Health 3:507–517.

McDonnell WF, Horstman DH, Hazucha MJ, Seal E Jr, Haak ED, Salaam SA, House DE. 1983. Pulmonary effects of ozone exposure during exercise: dose-response characteristics. J Appl Physiol 54:1345–1352.

McDonnell WF, Kehrl HR, Abdul-Salaam S, Ives PJ, Folinsbee LJ, Devlin RB, O'Neil JJ, Horstman DH. 1991. Respiratory response of humans

exposed to low levels of ozone for 6.6 hours. Arch Environ Health 46:145–150.

McDonnell WF, Stewart PW, Andreoni S, Seal E Jr, Kehrl HR, Horstman DH, Folinsbee LJ, Smith MV. 1997. Prediction of ozone-induced FEV1 changes. Effects of concentration, duration, and ventilation. Am J Respir Crit Care Med 156:715–722.

McDonnell WF, Stewart PW, Smith MV. 2007. The temporal dynamics of ozone-induced FEV1 changes in humans: an exposure-response model. Inhal Toxicol 19:483–494.

McDonnell WF, Stewart PW, Smith MV. 2010. Prediction of ozone-induced lung function responses in humans. Inhal Toxicol 22:160–168.

McDonnell WF, Stewart PW, Smith MV, Pan WK, Pan J. 1999. Ozone-induced respiratory symptoms: exposure-response models and association with lung function. Eur Respir J 14:845–853.

Schelegle ES, Adams WC, Giri SN, Siefkin AD. 1989. Acute ozone exposure increases plasma prostaglandin F2 alpha in ozone-sensitive human subjects. Am Rev Respir Dis 140:211–216.

Schelegle ES, Morales CA, Walby WF, Marion S, Allen RP. 2009. 6.6-hour inhalation of ozone concentrations from 60 to 87 parts per billion in healthy humans. Am J Respir Crit Care Med 180:265–272.

Schelegle ES, Walby WF, Adams WC. 2007. Time course of ozone-induced changes in breathing pattern in healthy exercising humans. J Appl Physiol 102:688–697.

Seal E Jr, McDonnell WF, House DE, Salaam SA, Dewitt PJ, Butler SO, Green J, Raggio L. 1993. The pulmonary response of white and black adults to six concentrations of ozone. Am Rev Respir Dis 147:804–810.

Silverman F, Folinsbee LJ, Barnard J, Shephard RJ. 1976. Pulmonary function changes in ozone-interaction of concentration and ventilation. J Appl Physiol 41:859–864.